IJARSCT
ISSN (Online) 2581-9429
International Journal of Advanced Research in Science, Communication and Technology (IJARSCT)
International Open-Access, Double-Blind, Peer-Reviewed, Refereed, Multidisciplinary Online Journal
Impact Factor: 7.301
Volume 3, Issue 5, June 2023

Thermopower in 3D Dirac Semimetal Na_3Bi

Kasala Suresha
Department of Physics
Government First Grade College, Davanagere, India
kasalasuresha@rediffmail.com

Abstract: *We study the electronic contribution to the thermopower of 3D Dirac semimetal using a semiclassical Boltzmann approach. We investigate the effect of various relaxation processes including disorder and interactions on the thermoelectric properties. We find that the thermopower have an interesting dependence on the chemical potential that is characteristic of the linear electronic dispersion, and that the electron-electron interactions modify the Lorenz number. We observed the dependence of thermopower on electron temperature and conclude that thermopower has higher values for electron-electron scattering as compared to charged impurity and short range disorder scattering mechanisms.*

Keywords: Thermopower, charged impurities, electron-electron interaction, short range disorder, Dirac semimetal, Na_3Bi

I. INTRODUCTION

In the past few years, the discoveries of graphene and topological insulators (TIs) have sparked enormous interest in the research of Dirac and topological quantum materials [1]. Graphene is a single sheet of carbon atoms that possess 2D Dirac fermions in its electronic structure [2] and TIs are materials with bulk energy gap but gapless surface states formed by an odd number of Dirac fermions with helical spin texture [3]. With the swift development in both fields, questions, such as whether there exists a 3D counterpart of graphene, and whether there exist different materials (other than insulators) that can possess unusual topology in their electronic structures, were naturally raised. Interestingly, the answers to both questions can lie in a same type of novel quantum matter – the topological Dirac semimetal. In a topological Dirac semimetal, the bulk conduction and valance bands contact only at discrete (Dirac) points and disperse linearly along all (three) momentum directions, forming bulk (3D) Dirac fermions – this naturally makes it the 3D counterpart of graphene. Remarkably, although the point-touching electronic structure has been discussed since more than seven decades ago [4], its topological classification was only appreciated recently [5,6] leading to the theoretical proposal of topological Dirac semimetals. The distinct electronic structure of a topological Dirac semimetal not only makes it possible to realize the many exciting phenomena and applications of graphene [7] in 3D materials, but also gives rise to many unique properties, such as the giant diamagnetism that diverges logarithmically when the Fermi-energy (EF) is approaching the 3D Dirac point [8,9], quantum magnetoresistance showing linear field dependence in the bulk [10,11], unique Landau level structures under strong magnetic field and oscillating quantum spin Hall effect in its quantum well structure [12]. Interestingly, the 3D Dirac Fermion in a topological Dirac semimetal is composed of two overlapping Weyl fermions (which are chiral massless particles previously studied extensively in high-energy physics, e.g. as a description of neutrinos) that can be separated in the momentum space - if time reversal or inversion symmetry is broken form the topological Weyl semimetal, another novel topological quantum state showing unique Fermi-arcs geometry [13], exhibiting pressure induced anomalous Hall effect [14] and quantized anomalous Hall effect in its quantum well structure [13].

Unfortunately, despite these strong motivations, the realization of the topological Dirac semimetal is challenging. In principle, it may be accidentally realized through topological phase transitions, such as tuning chemical composition or spin-orbital coupling strength to the quantum critical point through a normal insulator - topological insulator transition. However, such accidental realization is fragile, as the exact chemical composition is hard to control and sensitive to synthesis conditions; and the spin-orbital coupling strength in different materials is not a continuously tunable parameter. Recently, it was realized that the crystal symmetry may protect and stabilize 3D Dirac points and several stoichiometric compounds have been -cristobalite BiO_2 [5] and A_3Bi β theoretically proposed as topological Dirac

IJARSCT
ISSN (Online) 2581-9429
International Journal of Advanced Research in Science, Communication and Technology (IJARSCT)
International Open-Access, Double-Blind, Peer-Reviewed, Refereed, Multidisciplinary Online Journal
Impact Factor: 7.301
Volume 3, Issue 5, June 2023

semimetals, such as -cristobalite BiO_2,β (A=Na, K, Rb) family of compounds. [6]. Due to the metastable nature we chose Na_3Bi as the subject of study in this work.

Recently there has been a surge of interest in Dirac Semimetals and Weyl semimetals [15,16], as they evince many topological transport and optical properties not shared by other 3D materials. Weyl semimetals exhibit anomalous Hall and Nernst effects [17,18] , while dynamic chiral magnetic effect can be related to optical gyrotropy and natural optical activity in inversion broken Weyl semimetals. More interestingly, the surface of Weyl semimetals hosts distinct Fermi arcs, and the bulk transport is characterized by negative longitudinal magnetoresistance in the presence of parallel electric and magnetic fields due to chiral anomaly [19,20]. Very recently, the current authors along with others, proposed the planar Hall effect (PHE) as another striking consequence of chiral anomaly in WSMs, where the effect manifests itself when the applied current, magnetic field, and the induced transverse Hall voltage all lie in the same plane, precisely in a configuration in which the conventional Hall effect vanishes. This resulted in a series of experiments, where this effect was confirmed by several groups [21,22] in Weyl and Dirac semimetals. Even though the anomalous Nernst effect should vanish in a continuum model of Weyl fermions, it was shown to be both non-vanishing and measurable in both Dirac and Weyl semimetals [23]. In fact, a large Nernst signal has been experimentally measured in both Dirac42 and Weyl semimetals [24], which primarily arises due to the giant Berry curvature of the Bloch bands and the Dirac dispersion, respectively. The predicted Nernst effect strictly falls into the category of anomalous or conventional Nernst response. An anomalous (conventional) Nernst effect requires the presence of Berry curvature (magnetic field) in a direction perpendicular to the plane of temperature gradient and the induced voltage. Here, we propose another type of Nernst effect, namely the planar Nernst effect (PNE), which strictly arises as a consequence of chiral anomaly, and displays properties distinct from both the conventional and anomalous Nernst effects. The planar Nernst effect can be also viewed as transverse thermopower, analogous to the conventional thermopower (Seebeck coefficient) where a thermal gradient induces a thermoelectric voltage. In the current scenario, the voltage is induced transverse to the thermal gradient. The effect is shown to manifest in a configuration when the applied temperature gradient, magnetic field, and the induced voltage are co-planar. The planar Nernst effect is known to occur in ferromagnetic systems [25], however to the best of our knowledge has not been explored in WSMs/DSMs. We develop a quasi-classical theory of the planar Nernst effect in Weyl and Dirac semimetals, where the Fermi surfaces enclose nonzero fluxes of the Berry curvature in momentum space. Our findings, specifically a 3D map of the planar Nernst coefficient in type-I (Na_3Bi, Cd_3As_2 etc) and type-II Dirac semimetals (VAI_3, $PdTe_2$ etc), can be verified experimentally by an in-situ 3D double-axis.

II. THEORY

In this section we investigate the electronic contributions to the thermal conductivity and thermopower in the absence of a magnetic field of a single Weyl node, with a given chirality, described by the following Hamiltonian

$$H = \chi \hbar v_f \boldsymbol{\sigma} * \boldsymbol{k} \qquad (1)$$

where χ is the chirality that takes values of ± 1, v_f is the Fermi velocity, $\boldsymbol{\sigma} = \{\boldsymbol{\sigma}_x, \boldsymbol{\sigma}_y, \boldsymbol{\sigma}_z\}$ is a vector of Pauli matrices, and $\boldsymbol{k}$ is the wavevector. Our fundamental physical conclusions are not changed if the velocity is different in different directions, though asymmetric transport properties will result. To generalize to an arbitrary number of Weyl nodes, one simply adds the conductivity for each node together, provided one is able to ignore inter-node scattering which may open a gap [26]. If the Fourier component of the scattering potential is "small" at the wave vector connecting the nodes, this can be safely done. While disorder may gap a Dirac node (two Weyl nodes "on top" of each other), if the Fermi energy is larger than the gap induced in the node the system will remain metallic with an approximately linear dispersion. We will assume this is the case throughout this work. For relaxation through electronelectron interactions, zero wave vector scattering is insensitive to chirality [27] and as such, our results for electron-electron interactions apply to both Dirac and Weyl semimetals. To obtain the thermoelectric coefficients for a single Dirac node, one must add the results of two Weyl nodes with opposite chirality together.

In our work, we ignore contributions to the thermoelectric coefficients from phonons, which are expected to dominate thermal transport above the Debye temperature [28]. In this situation, one would add the phonon (or even magnon) contributions to the electronic one to find the total thermal conductivity.

IJARSCT
ISSN (Online) 2581-9429
International Journal of Advanced Research in Science, Communication and Technology (IJARSCT)
International Open-Access, Double-Blind, Peer-Reviewed, Refereed, Multidisciplinary Online Journal
Impact Factor: 7.301
Volume 3, Issue 5, June 2023

We obtain f^{χ} by solving the Boltzmann equation [29] which is given by (in the absence of magnetic fields)

$$\frac{\partial f^{\chi}}{\partial t} + \{(v + eE \times \Omega^{\chi}) * \nabla_r f^{\chi} + eE * \nabla_k f^{\chi}\} = I^{\chi}_{coll} \qquad (2)$$

where I^{χ}_{coll} is the collision integral at the Weyl node with chirality χ. The temperature gradient (which we take to define the x-direction) and electric field are taken to be in the x−direction, which allows us to drop the $E \times \Omega^{\chi}$ term since the spatial gradient of the distribution function is parallel to the thermal gradient. We solve the Boltzmann equation, via the relaxation time approximation, in which case the collision integral takes the form $I^{\chi}_{coll} = -\frac{f^{\chi} - f_{eq}}{\tau}$, where τ(k) is the intra-node scattering time. Following Ref. [28], we assume the following steady-state solution for the distribution function

$$f^{\chi} = f_{eq} + \tau(\varepsilon(k))\left(-\frac{\partial feq}{\partial \epsilon}\right) v * \left(-eE + \frac{\epsilon(k) - \mu}{T}(-\nabla \mathrm{T})\right) \qquad (3)$$

valid in the linear response regime.

2.1 Charged Impurities

We first calculate the transport coefficients for scattering off charged impurities, which lead to dopants in the band structure and move the Fermi level away from the nodal point. The transport time was computed in the first Born approximation in the work of Burkov, Hook, and Balents [30] They used a screened Coulomb potential given by

$$V(q) = \frac{4\pi e^2}{\epsilon_d (q^2 + q^2_{TF})} \qquad (4)$$

where $q^2_{TF} = \frac{4\pi e^2}{\epsilon_d} g(\epsilon)$ is the Thomas-Fermi wave vector and ϵ_d is the background dielectric constant. We note that a more accurate dielectric function with logarithmic corrections has 5 been worked out in Ref. [31] by evaluating the polarization bubble. However, in the following we will neglect those corrections. BHB found the scattering time to be

$$\frac{1}{\tau_{scr}(\epsilon)} = \frac{4\pi^3 n_i \hbar^2 v_f^3}{3\epsilon^2} f(\alpha) \qquad (5)$$

where n_i is the density of charged impurities and

$$f(\alpha) = \frac{3\alpha^2}{\pi^2}\left\{\left(1 + \frac{\alpha}{\pi}\right) \operatorname{atanh}\left(\frac{1}{1+\frac{\alpha}{\pi}}\right) - 1\right\} \qquad (6)$$

where $\alpha = \frac{e^2}{\epsilon_d v_f}$ and is the ratio of Coulomb (potential) energy to kinetic energy. We assume the charged impurities act as donors, so that $\epsilon_f \propto v_f n_i^{1/3}$. $f(\alpha)$ arises from using Fermi's golden rule to calculate the transport time. Physically it measures the strength of the interaction between electrons and the charge impurities. Using Eq. (5) as the scattering time, (e.g. using the Sommerfeld expansion), we find

$$S = -\frac{4\pi^2}{3}\frac{k_B}{e}\frac{k_B T}{\epsilon_f}\left(1 - \frac{3\pi^2}{5}\left(\frac{k_B T}{\epsilon_f}\right)^2\right) \qquad (7)$$

2.2 Electron-Electron Interactions

If the concentration of charged impurities approaches zero, the Fermi energy will approach the Weyl node. In this limit, we no longer expect scattering off charged impurities to dominate the transport properties due to absence of charged impurities to scatter electrons. At neutrality (and assuming there are no impurities present to dope the system), one instead expects electron-electron interactions to dominate relaxation processes due to the weak screening of the Coulomb interaction near the Fermi point, similar to graphene. This situation is in contrast to normal metals, i.e. Fermi liquids, where electron-electron interactions do not provide an efficient relaxation method even if they are strong. Near a Weyl point the only energy scale is the temperature, so the self energy is expected to be proportional to the temperature [27]. Thus, as pointed out in Ref. [27] the inverse scattering time for electron-electron interactions (when $0 \leq \mu < k_B T$) is (up to log corrections),

$$\frac{1}{\tau_{e-e}} = 2\, IM \sum = \frac{1}{A}\alpha^2 T \qquad (8)$$

IJARSCT
ISSN (Online) 2581-9429
International Journal of Advanced Research in Science, Communication and Technology (IJARSCT)
International Open-Access, Double-Blind, Peer-Reviewed, Refereed, Multidisciplinary Online Journal
Impact Factor: 7.301
Volume 3, Issue 5, June 2023

where A is a proportionality constant. We note for $\mu > k_BT$, the self-energy is proportional to the energy of the quasi-particle, not the temperature [30]. The relaxation time for electron-electron interactions can also be worked out explicitly from field theoretical methods, as was done in Ref. [30]. Using Eq. (8) as the scattering time, we find

$$S = -2\frac{k_B}{e}\frac{\varepsilon_f}{k_BT}\left[1 - \frac{3}{\pi^2}\left(\frac{\varepsilon_f}{k_BT}\right)^2\right] \quad (9)$$

2.3 Short-Range Disorder

We finish with the case of short range disorder, which is less realistic for Weyl and Dirac semimetals because the relatively poor screening of charged impurities (the most likely type) will lead to longer-range potentials. Nevertheless, it is useful to investigate the predictions for the thermal properties in this case for purposes of comparison. We ignore rare region effects, [26] which give rise to a exponentially small density of states at the Weyl node. Again, the scattering time was calculated in the first Born approximation, which is valid for weak disorder,

$$\frac{1}{\tau_{disorder}} = 2\pi\gamma g(\epsilon) \quad (10)$$

where $\gamma = u_0^2 n_d$ and n_d is the concentration of impurities. Ref. [32] noted that this was the state lifetime and including vertex corrections introduces a factor of (3/2) between the state lifetime and the transport time, i.e. $\tau_{tr} = \frac{3}{2}\tau$. In this section, we use the transport time to obtain the thermoelectric coefficients. One expects disorder to dominate near the Weyl point, at high temperatures, in which case the energy, $\epsilon = k_BT$. Using Eq. (10) for the relaxation time, we find

$$S = -\frac{5}{24}\frac{\gamma^2}{v_f^6\hbar^6}\frac{k_B}{e}k_BT\epsilon_f \quad (11)$$

to lowest order in disorder strength. As in the case of relaxation due to charged impurities, the Wiedemann-Franz law holds for relaxation due to weak short-range disorder. We note that for strong disorder, there is a crossover to diffusive behavior [33]. The transition to diffusive behavior is beyond the scope of this paper and cannot be captured within the first Born approximation.

III. RESULTS AND DISCUSSION

Before studying the effect of electric fields on the thermal transport, we briefly compare our zero-field results to each other and contrast our results with other phases of matter that do not possess the three-dimensional linear dispersion. First, the temperature dependence of the thermopower can be the same with respect to different scattering processes. As an explicit example of this, we see that the thermopower due to scattering off charged impurities has the same linear temperature dependence as scattering off short-range disorder. However, for scattering rates that are independent of the temperature, most common band structures, including quadratic band structures, will have the same linear temperature dependence, so this feature does not serve as an identifier of a Weyl or Dirac semimetal. Experimentally investigating the transport coefficients as a function of the Fermi energy (perhaps through gating a sample), would provide a clearer experimental signature of the Dirac or Weyl semimetal, compared to measuring the temperature dependence. Measuring just the longitudinal thermoelectric coefficients, would not allow one to distinguish between a Weyl or Dirac semimetal. We note that the quadratic temperature dependence of thermal conductivity is interesting when electron-electron interaction dominates relaxation processes since the scattering time then depends on the temperature. One experimental feature to look for in a three-dimensional system with linear electronic dispersion would be a crossover in the temperature dependence of the thermal conductivity from quadratic to linear upon adding/removing charged impurities (dopants) or disorder. Of course, in real materials transport will be determined by a mix of all scattering processes, and we expect Matthiessen's rule, $\frac{1}{\tau_{total}} = \frac{1}{\tau_i}$, where τ_i are the rates from different scattering processes, to apply, assuming these scattering processes can be treated as independent. We now discuss the regimes of validity for each scattering process. We begin with a clean Weyl semimetal with the Fermi level at the Weyl node, in which case the transport is determined by electron-electron interactions. We then imagine adding charged impurities, which change the Fermi energy. We can find the condition for scattering off charged impurities to dominate transport due to electron-electron interactions by comparing inverse scattering rates (assuming Fermi energy away from the nodal point): We now imagine adding short-range (uncharged) disorder to the system. Again comparing inverse scattering rates,

IJARSCT
ISSN (Online) 2581-9429
International Journal of Advanced Research in Science, Communication and Technology (IJARSCT)
International Open-Access, Double-Blind, Peer-Reviewed, Refereed, Multidisciplinary Online Journal
Impact Factor: 7.301
Volume 3, Issue 5, June 2023

scattering from short range impurities will dominate transport. This requires high enough temperatures to neglect electron-electron scattering, but also the condition $\frac{\hbar^6 v_f^6 n_i}{u_0^2 n_d \epsilon_f^4} f(\alpha) \ll 1$.

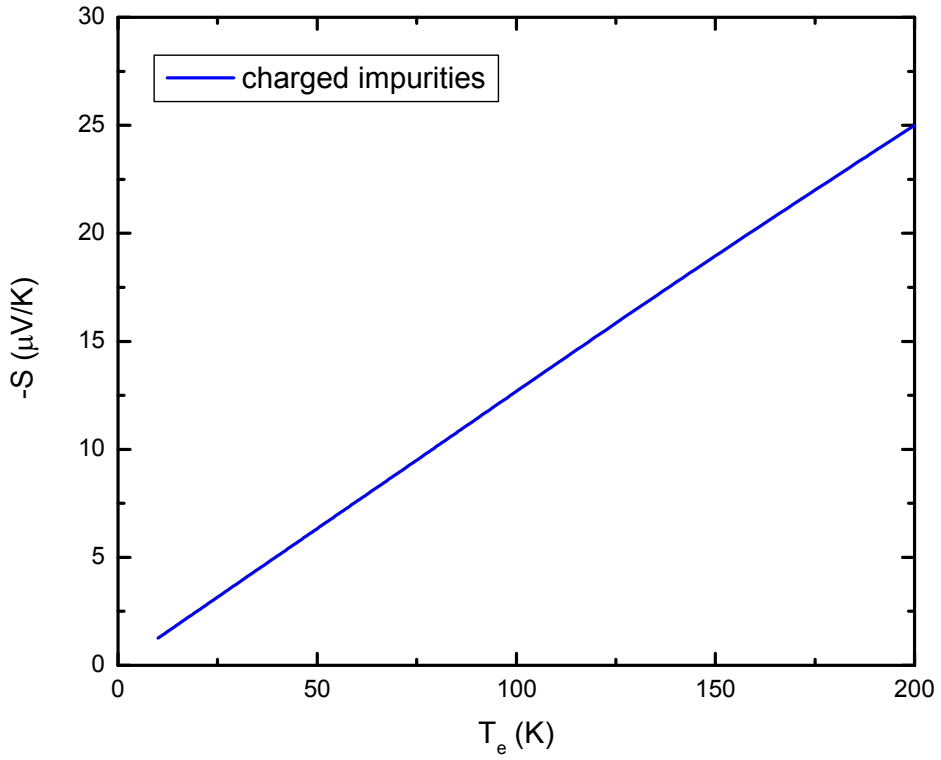

Figure 1: Variation of thermopower with electron temperature for n_i = 1.0x10^{18} m^{-3}

Figure 1 below shows the variation of thermopower with electron temperature and observed linear variation for charged impurity scattering mechanism. This linear behavior is also observed in many 3D Dirac semimetals. In our calculations we used characteristic materials parameters for Na_3Bi such as m* = 0.31m$_0$ and v_f= 5.10x10^5 m/s. We consider the carrier concentration n_i = 1.0x10^{18} m^{-3} in all our calculations.

For the electron-electron scattering mechanism, figure 2 below shows the variation of thermopower with electron temperature. We observed decrease of thermopower with temperature. At lower temperature, the thermopower decreases abruptly and at higher temperature, the decrements slows down and almost reaches zero at very high temperature. The value of thermopower we obtained as much larger in this electron-electron scattering as compared to charged impurity scattering, indicating the importance of electron-electron scattering mechanism in 3D Dirac semi metals.

In the presence of a magnetic field at finite charge density, a Dirac semimetal becomes a Weyl semimetal [34], thus our approach applies to both Weyl and Dirac semimetals, provided one can ignore inter-node scattering, as we discussed earlier. In our approach we treat the scattering time as a phenomenological parameter, i.e. we set the quasi-particle energy that appears in the scattering time equal to the chemical potential. Treating the scattering time as independent of quasi-particle energy is a valid assumption given that this semi-classical treatment is only valid at large chemical potential and the scattering times considered earlier decrease when the chemical potential increases. Stated more explicitly, whenever the scattering time appears, the integrand that determines the transport coefficients is centered around μ with its width proportional to $k_B T$ (due to the term with the derivative of f_{eq} with respect to energy)[35]. The scattering times we considered, which decrease rapidly with μ, do not change appreciably over this width given that our approach is only valid when $\mu \gg k_B T$.

IJARSCT
ISSN (Online) 2581-9429
International Journal of Advanced Research in Science, Communication and Technology (IJARSCT)
International Open-Access, Double-Blind, Peer-Reviewed, Refereed, Multidisciplinary Online Journal
Impact Factor: 7.301
Volume 3, Issue 5, June 2023

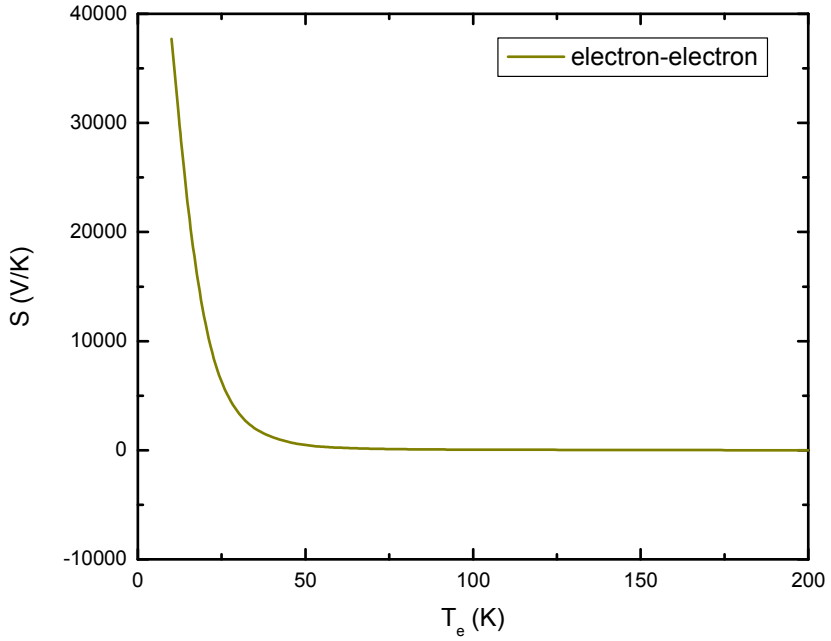

Figure 2: Variation of thermopower with electron temperature for n_i = 1.0x10^{18} m^{-3}

Thus, we are able to treat the scattering time phenomenologically. We also note that for the scattering times considered earlier when $\mu > T$ are independent of temperature. We stress in our model that the distance between the Weyl nodes is determined by the magnetic field. If the distance between the Weyl nodes is determined by something other than the magnetic field (which happens in stacked layers of three dimensional topological insulators and normal insulators for example), one expects the thermoelectric coefficients to have a different dependence on the magnetic field. Figure 3 is the variation of thermopower with electron temperature for the short range disorder scattering mechanism. We observed that the thermopower has very much lower as compared to charged impurity scattering. We also observed the thermopower has a linear dependence with temperature.

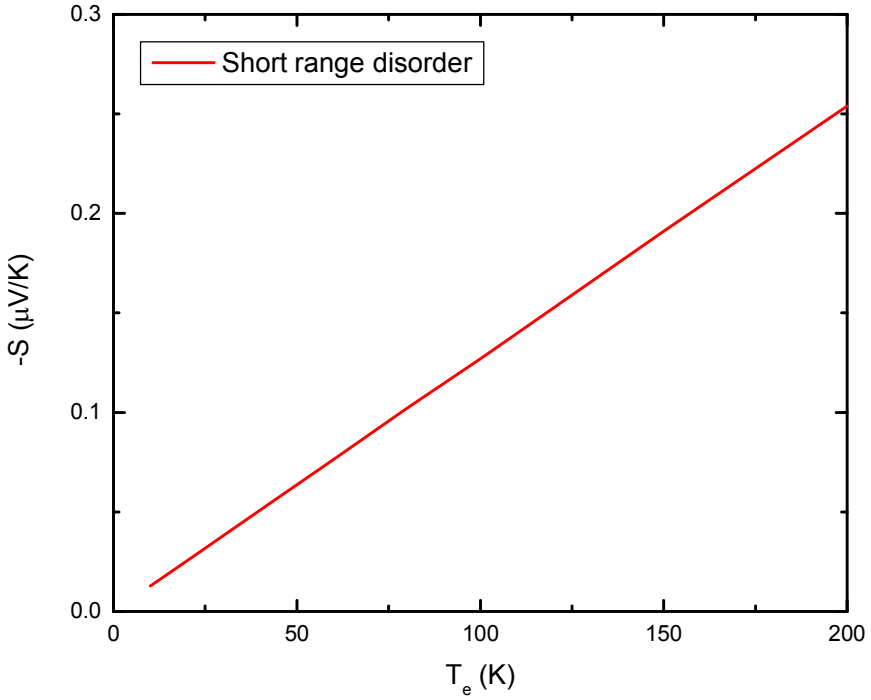

Figure 3: Variation of thermopower with electron temperature for n_i = 1.0x10^{18} m^{-3}

IJARSCT
ISSN (Online) 2581-9429
International Journal of Advanced Research in Science, Communication and Technology (IJARSCT)
International Open-Access, Double-Blind, Peer-Reviewed, Refereed, Multidisciplinary Online Journal
Impact Factor: 7.301
Volume 3, Issue 5, June 2023

IV. CONCLUSION

In our work, we have analytically investigated the electronic contribution to the thermoelectric properties of Dirac semimetals via the Boltzmann equation. We considered the cases where transport is relaxed by disorder and electron-electron interactions. We find an interesting dependence of the thermoelectric coefficients. Notably, in the case of interactions we find that the longitudinal thermal conductivity has interesting quadratic temperature dependence, in contrast to a linear dependence on the temperature for scattering from charged impurities that dope the system or short-range electrically neutral disorder. A linear temperature dependence of the thermal conductivity is the expected result for a "generic" metallic system (one without Weyl or Dirac points). We stress that in our work we have ignored the contribution from phonons to the thermal conductivity, which are expected to dominate at high enough temperatures. The lattice contributions are less generic than the electronic one. Notably, when the magnetic field and temperature gradient are parallel we find a large positive contribution to the longitudinal thermal conductivity that is quadratic in magnetic field strength, similar to the magnetic field dependence of the longitudinal electrical conductivity due to the presence of the chiral anomaly when there is no thermal gradient present, and there is a vanishing transverse thermal Hall conductivity. When the magnetic field is perpendicular to the temperature gradient, we find that the thermal conductivity is linear in magnetic field strength, and the longitudinal thermal conductivity picks up a negative contribution that goes as the square of the magnetic field. The presence of electric fields does not change these results under the assumption of no inter-node scattering.

REFERENCES

[1]. X.-L. Qi, S.-C. Zhang, Rev. Mod. Phys. **83**, 1057 (2011)
[2]. K. S. Novoselov et al., Science, **306**, 666 (2004)
[3]. J. E. Moore, Nature **464**, 194 (2010)
[4]. C. Herring, Phys. Rev. **52**, 365 (1937)
[5]. S. M. Young et al., Phys. Rev. Lett. **108**, 140405 (2012).
[6]. Z. Wang et al., Phys. Rev. B **85**, 195320 (2012)
[7]. A. K. Geim, Science **324**, 1530 (2009)
[8]. M. Koshino, T. Ando, Phys. Rev. B, **81**, 195431 (2010).
[9]. E. Röber, K. Hackstein, H. Coufal, S. Sotier, Phys. Status Solidi B, **93**, K99 (1979)
[10]. A. A. Abrikosov, Phys. Rev. B, **58**, 2788 (1998).
[11]. W. Zhang et al., Phys. Rev. Lett., **106**, 156808 (2011)
[12]. C.-X. Liu et al., Phys. Rev. B **81**, 041307 (2010)
[13]. G. Xu, H. Weng, Z. Wang, X. Dai, Z. Fang, Phys. Rev. Lett., **107**, 186806 (2011)
[14]. K.-Y. Yang, Y.-M. Lu, Y. Ran, Phys. Rev. B, **84**, 075129 (2011)
[15]. L. Lu, Z. Wang, D. Ye, L. Ran, L. Fu, J. D. Joannopoulos, and M. Soljacic, Science **349**, 622 (2015).
[16]. Z. J. Wang, Y. Sun, X. Q. Chen, C. Franchini, G. Xu, H. M. Weng, X. Dai and Z. Fang, Phys Rev B **85**, 195320 (2012).
[17]. Y. Ferreiros, A. A. Zyuzin, and J. H. Bardarson, Phys. Rev. B **96**, 115202 (2017).
[18]. M. N. Chernodub, A. Cortijo, and M. A. H. Vozmediano, Phys. Rev. Lett. **120**, 206601 (2018)
[19]. S. Liang, J. Lin, S. Kushwaha, J. Xing, N. Ni, R. J. Cava, and N. P. Ong, Phys. Rev. X **8**, 031002 (2018).
[20]. G. Sharma, P. Goswami, and S. Tewari, Phys. Rev. B **96**, 045112 (2017)
[21]. P. Li, C. H. Zhang, J. W. Zhang, Y. Wen, and X. X. Zhang, Phys. Rev. B **98**, 121108(R) (2018).
[22]. D. D. Liang, Y. J. Wang, W. L. Zhen, J. Yang, S. R. Weng, X. Yan, Y. Y. Han, W. Tong, L. Pi, W. K. Zhu, C. J. Zhang, arXiv:1809.01290v1 (2018).
[23]. G Sharma, C Moore, S Saha, S Tewari, Phys. Rev. B **96**, 195119 (2017)
[24]. S. J. Watzman, T. M. McCormick, C. Shekhar, S.-C. Wu, Y. Sun, A. Prakash, C. Felser, N. Trivedi, and J. P. Heremans, Phys. Rev. B **97**, 161404 (2018)
[25]. A. D. Avery, M. R. Pufall, B. L. Zink, Phys. Rev. Lett. **109**, 196602 (2012)
[26]. R. Nandkishore, D. A. Huse, and S. L. Sondhi, Phys. Rev. B **89**, 245110 (2014)
[27]. P. Hosur, S. A. Parameswaran, and A. Vishwanath, Phys. Rev. Lett. **108**, 046602 (2012)

IJARSCT
ISSN (Online) 2581-9429
International Journal of Advanced Research in Science, Communication and Technology (IJARSCT)
International Open-Access, Double-Blind, Peer-Reviewed, Refereed, Multidisciplinary Online Journal
Impact Factor: 7.301
Volume 3, Issue 5, June 2023

[28]. N. Ashcroft and N. Mermin, Solid State Physics (Sauners College, Philadelphia, (1976)
[29]. T. Qin, Q. Niu, and J. Shi, Phys. Rev. Lett. **107**, 236601 (2011)
[30]. A A. Burkov, M. D. Hook, and L. Balents, Phys. Rev. B **84**, 235126 (2011)
[31]. M. Lv and S.-C. Zhang, International Journal of Modern Physics B **27**, 1350177 (2013)
[32]. R. R. Biswas and S. Ryu, Phys. Rev. B **89**, 014205 (2014)
[33]. B. Sbierski, G. Pohl, E. J. Bergholtz, and P. W. Brouwer, Phys. Rev. Lett. **113**, 026602 (2014).
[34]. E. V. Gorbar, V. A. Miransky, and I. A. Shovkovy, Phys. Rev. B **88**, 165105 (2013)
[35]. N. Ashcroft and N. Mermin, Solid State Physics (Sauners College, Philadelphia, (1976))